Tip Clearance Effect on Through-Flow and Performance of a Centrifugal Compressor

Hark-Jin Eum*, Young-Seok Kang, Shin-Hyoung Kang
Turbo System & Control Laboratory, School of Mechanical and Aerospace engineering, Seoul National University, Seoul 151-742, Korea

Numerical simulations have been performed to investigate tip clearance effect on through-flow and performance of a centrifugal compressor which has the same configuration of impeller with six different tip clearances. Secondary flow and loss distribution have been surveyed to understand the flow mechanism due to the tip clearance. Tip leakage flow strongly interacts with mainstream flow and considerably changes the secondary flow and the loss distribution inside the impeller passage. A method has been described to quantitatively estimate the tip clearance effect on the performance drop and the efficiency drop. The tip clearance has caused specific work reduction and additional entropy generation. The former, which is called inviscid loss, is independent of any internal loss and the latter, which is called viscous loss, is dependent on every loss in the flow passage. Two components equally affected the performance drop as the tip clearances were small, while the efficiency drop was influenced by the viscous component alone. The additional entropy generation was modeled with all the kinetic energy of the tip leakage flow. Therefore, the present paper can provide how to quantitatively estimate the tip clearance effect on the performance and efficiency.

Key Words : Tip Clearance, Through-Flow, Performance, Centrifugal Compressor, Secondary Flow, Loss Distribution, Tip Leakage Flow, Performance Drop, Efficiency Drop, Specific Work Reduction, Additional Entropy Generation, Kinetic Energy

Nomenclature

C_p : Specific heat at constant pressure
C_θ : Absolute circumferential velocity
C_m : Absolute meridional velocity
p_o : Total pressure
R : Universal gas constant
T_o : Total temperature
W : Relative velocity
h_o : Total enthalpy
$\dot{m}$: Mass flow rate
s : Entropy
t : Tip clearance
u : Impeller speed
v : Velocity

Greek symbols

β : Relative flow angle
γ : Specific heat ratio
η : Efficiency
π : Total to total pressure ratio, p_{o2}/p_{o1}
τ : Total to total temperature ratio, T_{o2}/T_{o1}
ζ : Viscous loss factor
Δ : Increment

Subscripts

1 : Impeller inlet
2 : Impeller exit
m : Meridional direction
n : Normal direction in blade
l : Leakage flow
lm : Leading edge of main blade
tm : Trailing edge of main blade

* Corresponding Author,
E-mail : eum@turbo.snu.ac.kr
TEL : +82-2-880-7118; **FAX** : +82-2-883-0179
Turbo System & Control Laboratory, School of Mechanical and Aerospace engineering, Seoul National University, Seoul 151-742, Korea. (Manuscript **Received** April 8, 2003; **Revised** February 20, 2004)

ls : Leading edge of splitter
ts : Trailing edge of splitter

Superscript
$*$: Value for zero tip clearance

1. Introduction

A gap exists between a rotating impeller and a stationary wall in unshrouded axial or centrifugal compressors. The gap is called tip clearance. Leakage flow through the tip clearance is called tip leakage flow and is unavoidable in such compressors. The tip leakage flow has serious effect on the performance and efficiency. The effect is much more deleterious in centrifugal compressors than axial compressors because a centrifugal compressor has a long narrow flow passage so that the tip clearance occupies a large portion of the flow passage. Many researches have been carried out on flow mechanism, flow structure and performance loss due to the tip leakage flow. The mechanism of the tip leakage flow has been known to be primarily inviscid, because overall magnitude of the tip leakage flow remains strongly related to the aerodynamic loading of the blade (Rains, 1954; Storer and Cumpsty, 1991). It has been elucidated experimentally and numerically that leakage flow alters the secondary flow pattern and distribution of the low momentum fluid so that the tip clearance loss accounts for nearly 20-40% of the total losses (Lakshminarayana, 1970; Moor et al., 1984; Farge et al., 1989; Hah, 1986; Larosiliere et al., 1999; Myong and Yang, 2003). However, it is still required to figure out how the tip leakage flow contributes to the performance drop or the efficiency drop. Several models (Rains, 1954; Pampreen, 1973; Senoo and Ishida, 1986; Senoo and Ishida, 1987; Ishida et al., 1990) have been proposed to predict the pressure loss and the efficiency drop due to the tip clearance in centrifugal and axial compressors. However, they still need several empirical constants which need to be tuned and depend on the configuration of the impellers. Further studies on the tip clearance effect are still necessary to understand the loss mechanism and improve the performance.

This paper attempts to gain further insight into three-dimensional complex flow stirred by the tip leakage flow and find a linkage of the complex flow with the performance drop and the efficiency drop one-dimensionally. The same configuration of centrifugal compressor impeller with six different tip clearances has been employed for numerical simulations, for which a commercial CFD code, CFX-TASC flow, is used. To begin with, the secondary flow and loss distribution are checked to understand the complex flow stirred by the tip leakage flow. One-dimensional approach is followed to find the linkage of the complex flow with the performance drop and the efficiency drop and also to estimate how much the effect of the tip leakage flow is.

2. Numerical Method and Impeller Model

CFX-TASC flow, which is a commercially available CFD software, was used for the present numerical simulation. The code was developed for the turbomachinery flow simulations with multiple frames of reference and solves three-dimensional Reynolds-averaged Navier-Stokes equations in a primitive variable form. The turbulent flow is simulated with several two equations turbulence models. In the present study, the standard $k-w$ turbulence model is used because this model has shown a significantly more accurate prediction of separation in a number of test case and industrial applications (Choi, 1999). The centrifugal compressor impeller of an auxiliary power unit with vaned-diffuser was chosen for the present study. But the impeller with parallel wall vaneless diffuser was used to avoid an interaction between the impeller and the vaned-diffuser downstream of the impeller, because the interaction makes it difficult to estimate the effect of tip clearance alone on the performance (Shum et al., 2000). The tip clearance was made to have uniform gap from the leading edge to the trailing edge, while the blade heights were changed for each clearance in order to keep the flow passage area unchanged. Fig. 1 shows the meridional view

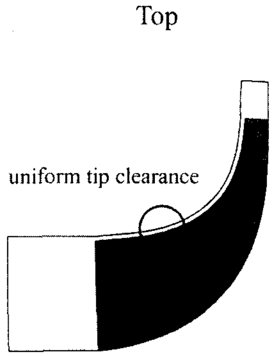

Fig. 1 Tip clearance uniformly distributed from the leading edge to the trailing edge of the impeller

of the impeller with uniformly distributed tip clearance from the leading edge to the trailing edge. Detailed specifications of the impeller and the design conditions are presented in Table 1. Six different tip clearances of 0.2, 0.3 0.5, 0.7, 0.9 and 1.1 mm were used for the numerical simulation. A zero tip clearance impeller with a stationary shroud was also simulated as a reference.

The CFX-TurboGrid was used for the generation of computational grid. Figure 2 shows the computational grid of H-type for a steady state simulation, including one main and one splitter blade. The nodes for the impeller consist of $86\times 49\times 36$points in streamwise, pitchwise and spanwise, respectively and 13 streamwise nodes were added for the parallel wall diffuser. Since the mechanism that the tip leakage flow occurs has been known to be intrinsically inviscid (Storer and Cumpsty, 1991) and especially the thickness of the impeller tip is very thin, a separation bubble doesn't occur on the impeller tip unlike the turbine blades so that many nodes are not required for the tip clearance (Shum, Tan and Cumpsty, 2000). Therefore, 4 to 9 nodes in the spanwise direction were assigned to the tip clearance.

The total pressure, total temperature and flow angle at the design condition were prescribed at the inflow boundary, while a mass flow rate was specified at the outflow boundary. The casing wall was stationary in the absolute frame of reference so that there was a relative motion between the casing and the impeller. All the solid walls were assumed to be adiabatic. All the calculations were carried out at the design flow rate condition specified in Table 1.

Table 1 Specification of the impeller

Mass flow rate	1.05 kg/s
Rotating Speed	60000 rpm
No. of blade (main+splitter)	13+13
Radius of impeller exit	82 mm
Outer radius of impeller inlet	54 mm
Inner radius of impeller inlet	28 mm
Backsweep angle of impeller	−25 deg
Tip clearance	0.0∼1.1 mm
Impeller exit height	6.4 mm

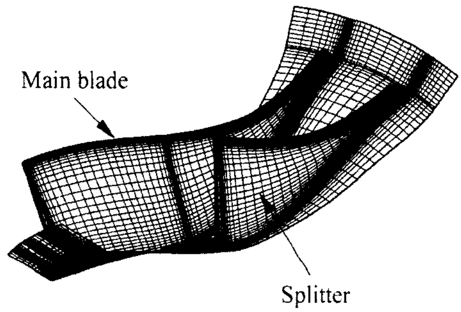

Fig. 2 Computational grid for the centrifugal compressor impeller

3. Flow Characteristics Inside the Impeller

Streamlines passing over the leading edge of the main blade and the splitter blade show well a secondary flow structure inside the passage as shown in Fig. 3. The secondary flow occurs near the suction surface of the blades, which then rolls up toward the shroud due to the pressure gradient, depending on the radius of the passage curvature between the hub and the shroud. A relative motion between the casing and the impeller moves the secondary flow to the pressure surface along the casing. At an impeller exit, a region through which the streamlines pass corresponds to a high loss region. Figure 4 shows the effect of

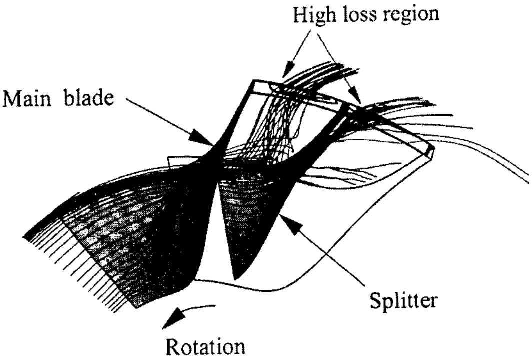

Fig. 3 Streamlines passing over the leading edge of the blade with zero tip clearance

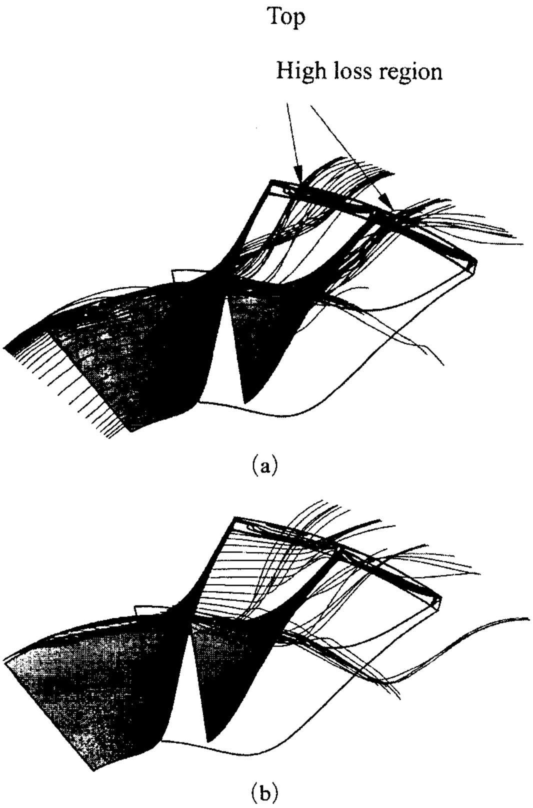

Fig. 4 Streamlines passing (a) Over the leading edge of the blade and (b) Through the tip clearance with 1.1 mm tip clearance

the tip leakage flow. The tip leakage flow changes the secondary flow structure and results in variation of the loss distribution at the impeller exit. The tip leakage flow leaving the leading edge of the main blade is developing into the tip leakage vortex and approaches to the leading edge of the splitter blade. Some pass over the next main blade once more and others pass the splitter blade, so that the loss distribution at the impeller exit considerably changes. The loss distribution at the impeller exit can be represented by the following loss factor, which is defined as an entropy generation throughout the passage, since the entropy generation at the impeller exit includes every loss throughout the passage (Koch and Smith, 1976; Whitfield et al., 1990; Denton, 1993).

$$\zeta = \exp(-\Delta s/R) \qquad (1)$$

Figures 5 and 6 show the loss factor distribution and the secondary flow at 45 % of the meridional length measured from the leading edge to the trailing edge of the impeller tip along the casing. For a zero tip clearance, high loss region concentrates in the suction/shroud corner as shown in Fig. 5(a), where the high loss region represents the region in which the loss factor is less than 0.9. The secondary flow shown in Fig. 5(b) is defined as the component of velocity normal to the primary flow. Near the blade surface, the flow has not enough momentum to overcome the pressure gradient toward the shroud from the hub, where the pressure gradient is developed by the centrifugal force acting on the flow passing the curved passage. As a result, the force by this pressure gradient pushes the flow toward the casing along the blade surface. Near the casing, the Coriolis force induces the secondary flow to move from the pressure surface (P.S) toward the suction surface (S.S), while the relative motion between the casing and the impeller induces the secondary flow in the opposite direction. The effect of the relative motion is much stronger in the right passage of the splitter blade than the left, because the flow gathered in the corner of the suction/shroud surface of the main blade from the hub has to continue to movs somewhere by an inertia effect so that the flow moves toward the pressure surface of the splitter blade by the relative motion. The high loss region corresponds to the region where a strong interaction occurs between the secondary flows flowing

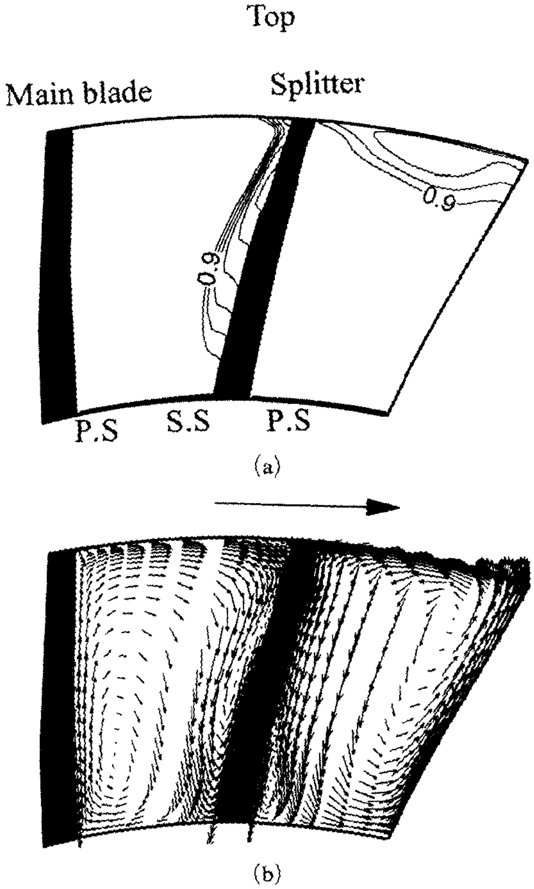

Fig. 5 (a) Loss factor and (b) Secondary flow at $l/s=0.45$ of zero tip clearance impeller

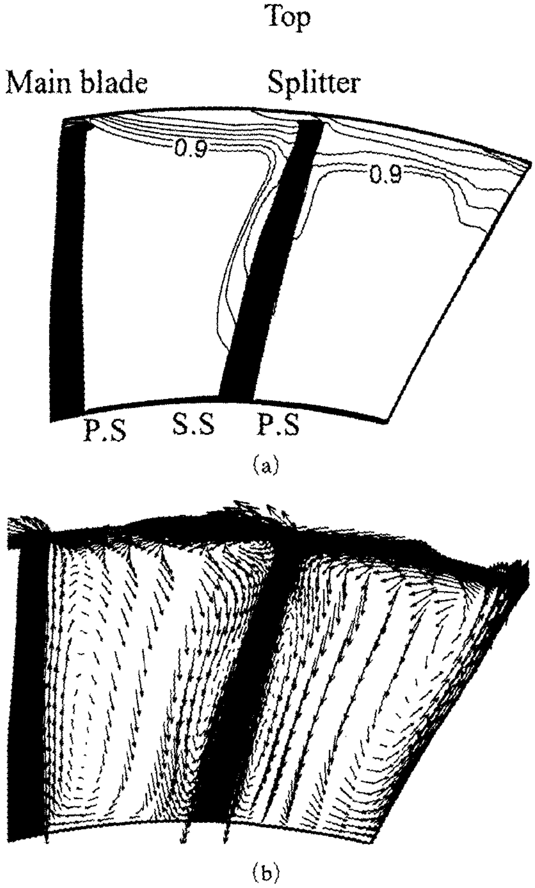

Fig. 6 (a) Loss factor and (b) Secondary flow at $l/s=0.45$ of 0.5 mm tip clearance impeller

in the opposite direction each other as shown in Fig. 5. Near the suction surface of the splitter blade, the interaction occurs between the clockwise secondary flow and the flow moving toward the casing from the hub along the suction surface. Near the casing of the right passage of the splitter blade, the interaction occurs between the secondary flow induced by the relative motion of the casing and the flow induced by the Coriolis force. On the other hand, when there is a tip leakage flow in the passage, the loss distribution and secondary flow show different behaviors as shown in Fig. 6, compared to those of zero tip clearance as shown in Fig. 5. High loss region occupies near the casing where there are very strong interactions between the tip leakage flow and the secondary flow as shown in Fig. 6(b).

The effect of the tip clearance on the loss is reflected at the impeller exit. Entropy generation at the impeller exit represents total loss accumulated throughout the passage. Figure 7 shows loss factors for the tip clearances at the impeller exit. Loss distributions at the impeller exit are considerably affected by the tip leakage flow. As the tip clearance increases, the high loss region near the suction surface of the splitter blade extends to the pressure surface of the main blade.

The total pressure, total temperature and entropy generation were averaged with mass flow rate at the cross sections of the impeller to examine the effect of the tip clearance on the performance and efficiency along the passage. Figure 8 shows variations of the decrement of the total-to-total pressure ratio relative to that of zero

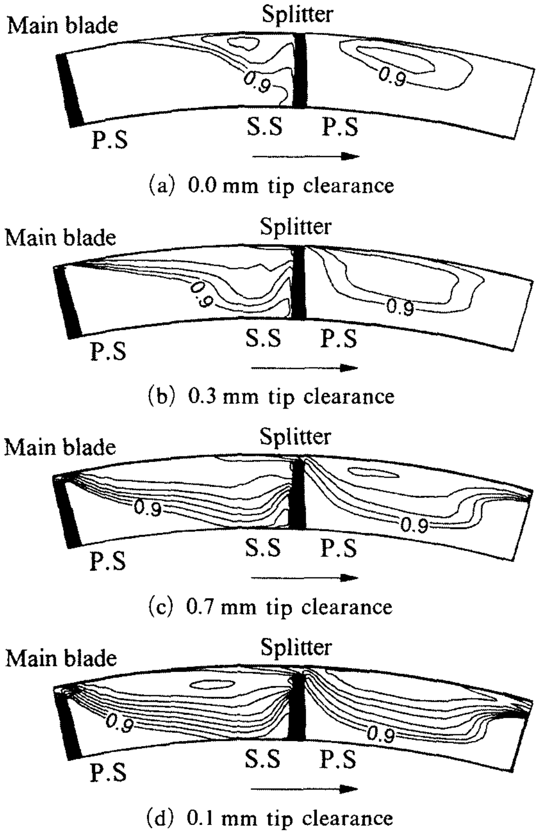

Fig. 7 Loss factor at the impeller exit

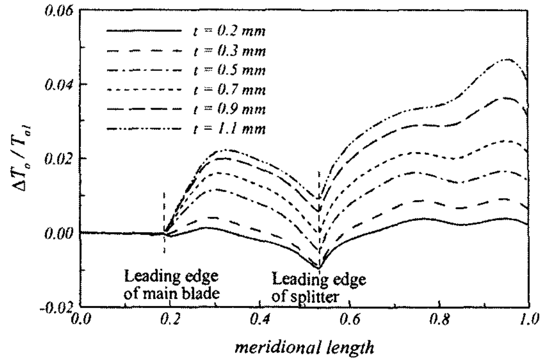

Fig. 9 Variations of total-to-total pressure ratio along the flow passage

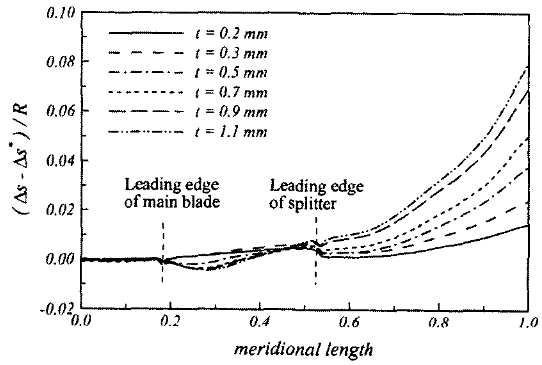

Fig. 10 Variations of additional entropy generation along the flow passage

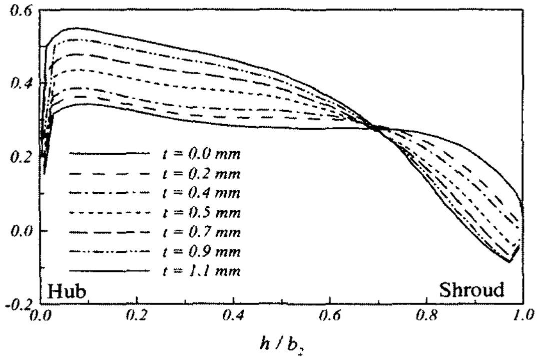

Fig. 11 Distributions of meridional component of absolute velocity at the impeller exit

tip clearance along the passage. As the tip clearance increases, the amount of the decrement of the total-to-total pressure ratio increases. However, it decreases a little between the leading edges of the main blade and the splitter blade for $t/b_2=0.2$ and $t/b_2=0.3$. This is also observed in Fig. 9 and 10. A favorable effect of the tip leakage flow is the reason. It has been known that the tip leakage flow rather reduces the secondary flow in the case of very small tip clearance (Cumpsty, 1989; Lakshminarayana, 1996). The additional entropy generation $(\Delta s-\Delta s^*)$ relative to the entropy generation of zero tip clearance increases steeply downstream of the impeller as shown in Fig. 10.

The tip leakage flow blocks the flow passage. It can be shown by the distribution of the radial component of velocity at the impeller exit as shown in Fig. 11. The increment of blockage decreases the radial velocity near the shroud and increases near the hub to satisfy the mass conservation. For large tip clearance, a reverse flow occurs near the shroud because the flow with low momentum does not overcome the pressure gradient in the radial direction. The total-to-total

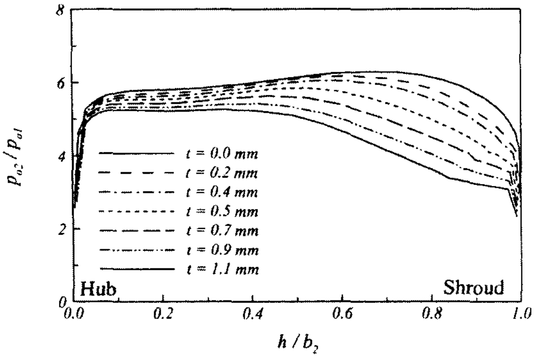

Fig. 12 Distributions of total-to-total pressure ratio at the impeller exit

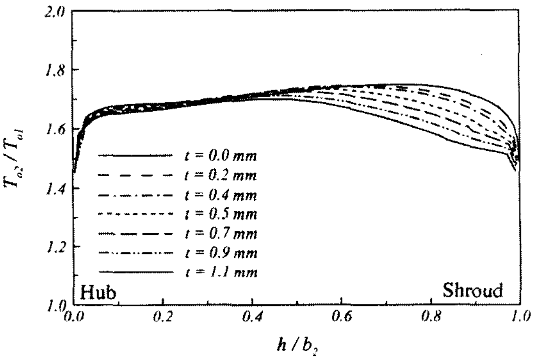

Fig. 13 Distributions of total-to-total temperature ratio at the impeller exit

pressure ratio and temperature ratio decrease mainly near the shroud as shown in Fig. 12 and 13. On the other hand, the variation of the total-to-total temperature ratio occurs only between the mid-span and the casing. This means that the tip leakage flow affects the work transferred by the impeller in this region.

4. Effects of the Tip Clearance

4.1 The performance drop

The one-dimensional equations are described based on the thermodynamic relations in order to find the linkage of the complex flow stirred by the tip leakage flow with the performance drop and the efficiency drop and also to estimate how much the tip clearance effect is. The total-to-total pressure ratio at the impeller exit, which represents the performance, can be presented with a function of total-to-total temperature ratio and the entropy generation as follows,

$$\pi=\tau^{\frac{\gamma}{\gamma-1}}\exp\left(-\frac{\Delta s}{R}\right)=\pi(\tau,\Delta s) \tag{2}$$

In Eq. (2), π denotes the total-to-total pressure ratio (p_{o2}/p_{o1}), τ the total-to-total temperature ratio (T_{o2}/T_{o1}) and Δs the entropy generation at the impeller exit. Using the Euler's equation (3), which defines the specific work done by the impeller and assuming no swirl of inflow ($C_{\theta 1}\approx 0$),

$$\Delta h_o=C_p(T_{o2}-T_{o1})=u_2C_{\theta 2}-u_1C_{\theta 1} \tag{3}$$

τ can be written as follows,

$$\tau=1+\frac{u_2C_{\theta 2}}{C_pT_{o1}} \tag{4}$$

In order to estimate the effect of the tip clearance on the performance, an incremental equation for the total-to-total pressure ratio relative to that of zero tip clearance is needed. If Eq. (2) is differentiated with respect to τ and Δs, Eq. (5) is obtained.

$$d\pi=\left.\frac{\partial\pi}{\partial\tau}\right)_{\Delta s}d\tau+\left.\frac{\partial\pi}{\partial\Delta s}\right)_{\tau}d\Delta s \tag{5}$$

After rearranging Eq. (5) using π^*, τ^* and Δs^* which are the total-to-total pressure ratio, the total-to-total temperature ratio and the entropy generation for zero tip clearance, respectively, the incremental equation becomes

$$\frac{\Delta\pi}{\pi^*}=\frac{\gamma}{\gamma-1}\frac{\Delta\tau}{\tau^*}-\frac{\Delta s-\Delta s^*}{R} \tag{6}$$

where $\Delta\pi=\pi-\pi^*$, $\Delta\tau=\tau-\tau^*$. The first term on the right hand side of Eq. (6) represents the variation of the specific work due to the tip leakage flow and the second term the additional entropy generation due to the viscous loss caused by the tip leakage flow. It can be considered that the first term is independent of the viscous loss of the flow inside the passage, because it comes from the energy and momentum equations alone (Japikse et al., 1994). Therefore, it is possible to decompose the loss of total pressure ($\Delta\pi/\pi^*$) due to the tip clearance into two components : the inviscid loss and the viscous loss. It can be assured in Fig. 14, where the symbol ○ represents

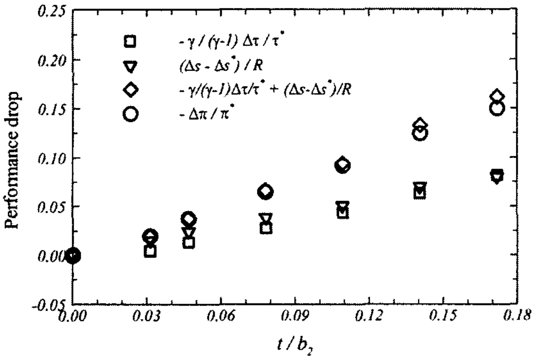

Fig. 14 Variations of total-to-total pressure drop due to the tip clearance relative to zero tip clearance

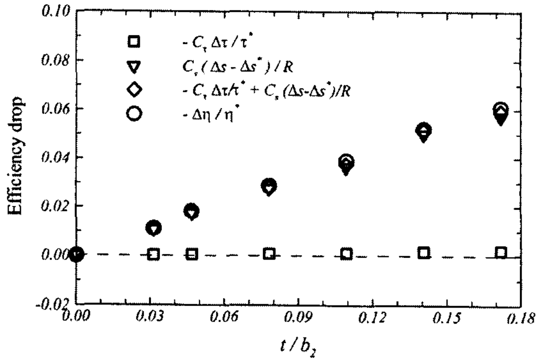

Fig. 15 Variations of efficiency drop due to the tip clearance relative to zero tip clearance

the loss of the total pressure ($\Delta\pi/\pi^*$) at the impeller exit due to the tip clearance and the symbol ◇ represents the summation of the inviscid loss (□) and the viscous loss (▽) on the right hand side of Eq. (6). They show good agreements with each other. As a result, the total pressure loss is affected by the viscous loss (▽) at the small tip clearances but equally affected by two components as the tip clearance increases; It is proportional to the ratio of the tip clearance to the blade exit height (t/b_2): $\Delta\pi/\pi^* \approx 0.88t/b_2$.

4.2 The efficiency drop

The isentropic efficiency can be described as a function of the total-to-total pressure and temperature ratios as follows.

$$\eta=\frac{h_{o2s}-h_{o1}}{h_{o2}-h_{o1}}=\frac{\pi^{\frac{\gamma-1}{\gamma}}-1}{\tau-1}=\eta(\pi,\ \tau) \tag{7}$$

If Eq. (7) is differentiated with respect to π and τ and then is rearranged with the incremental equation relative to the values of zero tip clearance, the following relations are obtained.

$$d\eta=\left.\frac{\partial\eta}{\partial\pi}\right)_\tau d\pi+\left.\frac{\partial\eta}{\partial\tau}\right)_\pi d\tau \tag{8}$$

$$\frac{\Delta\eta}{\eta^*}=\frac{\gamma-1}{\gamma}\left(1+\frac{1}{\pi^{*\frac{\gamma-1}{\gamma}}}-1\right)\frac{\Delta\pi}{\pi^*}-\frac{\tau^*}{\tau^*-1}\frac{\Delta\tau}{\tau^*} \tag{9}$$

If Eq. (6) is inserted into the first term of the right hand side of Eq. (9),

$$\begin{aligned}\frac{\Delta\eta}{\eta^*}&=\left(\frac{1}{\pi^{*\frac{\gamma-1}{\gamma}}-1}-\frac{1}{\tau^*-1}\right)\frac{\Delta\tau}{\tau^*}\\&\quad-\frac{\gamma-1}{\gamma}\left(1+\frac{1}{\pi^{*\frac{\gamma-1}{\gamma}}-1}\right)\frac{\Delta s-\Delta s^*}{R}\\&=C_\tau\frac{\Delta\tau}{\tau^*}-C_s\frac{\Delta s-\Delta s^*}{R}\end{aligned} \tag{10}$$

where the first parenthesis and the second of the right hand side are replaced with C_τ and C_s, respectively. Eq. (10) also decomposes the efficiency drop into two components of the inviscid loss and the viscous loss. As might be expected, the viscous loss alone influences the efficiency drop and the inviscid loss doesn't give any effect on the efficiency drop as shown in Fig. 15, where the symbol ○ represents the efficiency drop ($\Delta\eta/\eta^*$) at the impeller exit due to the tip clearance and the symbol ◇ represents the summation of the inviscid loss (□) and the viscous loss (▽) on the right hand side of Eq. (10). ; It is also proportional to the ratio to the tip clearance to the blade exit height: $\Delta\eta/\eta^* \approx 0.35t/b_2$.

4.3 The specific work drop

It was investigated in the previous section that the specific work was independent of the viscous loss inside the passage and influenced the performance drop. The specific work represents the work done per unit mass flow by the impeller and decreases as the tip clearance increases (Fig. 14 □). The variation of the specific work is associated with that of the total-to-total temperature ratio ($\Delta\tau=\tau-\tau^*$) and that of a circumferential

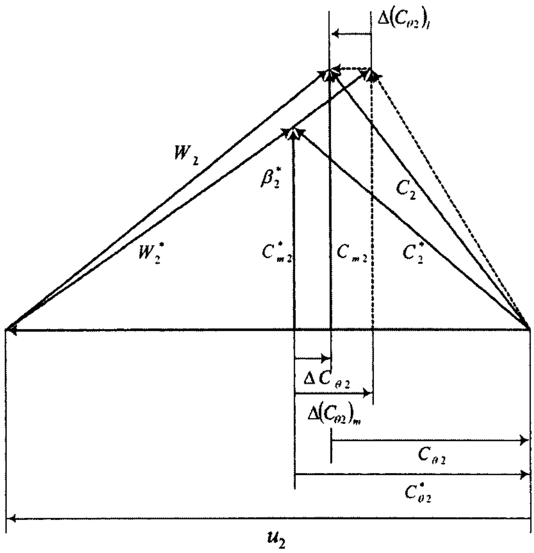

Fig. 16 Velocity triangle at the impeller exit

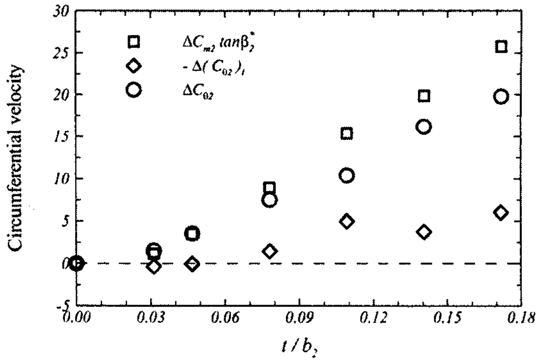

Fig. 17 Variations of circumferential component of absolute velocity due to the tip clearance at the impeller exit

component of absolute velocity ($\Delta C_{\theta 2}$) at the impeller exit as presented in Eq. (4). Therefore, it is convenient to present the variation of the specific work as the components of the absolute velocity at the impeller exit. That is, the total-to-total temperature ratio depends on the circumferential component of the absolute velocity ($C_{\theta 2}$) at the impeller exit when rotating speed and mass flow rate are constant. Here, $C_{\theta 2}$ is determined by the meridional component of the absolute velocity (C_{m2}) and slip velocity as illustrated in Fig. 16, which is a velocity triangle at the impeller exit. Since not only the static pressure and density decreases with the increase of tip clearance at the impeller exit but also the tip leakage flow blocks the flow passage, C_{m2} should increase with the tip clearance to satisfy the mass conservation for a constant mass flow rate. The slip of velocity occurs due to the tip leakage flow. Consequently, $\Delta C_{\theta 2}$ can be represented with the variation of C_{m2} and the slip velocity caused by the tip leakage flow as follows.

$$\begin{aligned}\Delta C_{\theta 2} &= \Delta(C_{\theta 2})_m + \Delta(C_{\theta 2})_l \\ &= \Delta C_{m2} \tan \beta_2^* + \Delta(C_{\theta 2})_l\end{aligned} \tag{11}$$

where β_2^* is the flow angle of the relative velocity for zero tip clearance at the impeller exit. Fig. 17 shows the variations of $\Delta C_{\theta 2}$ for each tip clearance. It is at small tip clearance that $\Delta C_{\theta 2}$(○) is affected by the variation of the meridional component of the absolute velocity (□) more than the slip velocity (◇) caused by the tip leakage flow. This means that the flow blockage is more important than the slip velocity due to the tip leakage flow at small tip clearance.

5. Model for Entropy Generation

The additional entropy generation ($\Delta s - \Delta s^*$) caused by the tip leakage flow represented the viscous loss throughout the passage and was the major source of the efficiency drop as presented in the previous section. If all the tip leakage flow are mixed with primary flow at the impeller exit, all the kinetic energy of the tip leakage flow will be dissipated into entropy generation by mixing process as follows.

$$\Delta s - \Delta s^* = \frac{1}{\dot{m} T_{o2}} \left(\int_{lm}^{tm} \frac{1}{2} v_n^2 d\dot{m}_l + \int_{ls}^{ts} \frac{1}{2} v_n^2 d\dot{m}_l \right) \tag{12}$$

The first term on the parenthesis of the right hand side represents the kinetic energy of the tip leakage flow integrated from the leading edge to the trailing edge of the main blade and the second that of the splitter blade. Fig. 18 shows the additional entropy generation (▽) and the kinetic energy of the tip leakage flow (□) for each ratio of the tip clearance to the blade exit height (t/b_2). They show good agreements with each other. This means that it is possible to

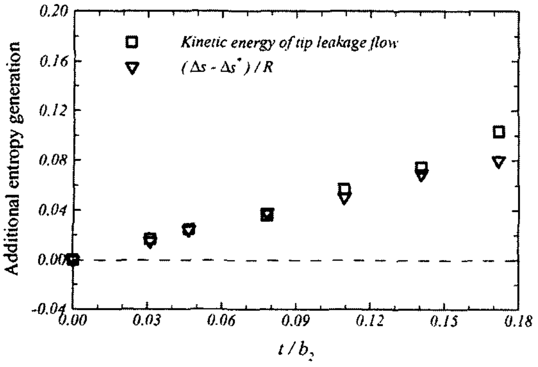

Fig. 18 Variations of additional entropy generation and kinetic energy of the tip leakage flow

predict the efficiency drop from the zero tip clearance using Eqs. (10) and (12) without any correlation at a design stage. In Eq. (12), v_n and $d\dot{m}_l$ are predictable using the inviscid mechanism of the leakage flow, where v_n is the leakage velocity component normal to the blade and $d\dot{m}_l$ the leakage mass flow rate, as presented by Rains (1954), Storer and Cumpsty (1991) and Senoo and Ishida (1986).

6. Conclusions

In order to investigate the effect of tip clearance on the through-flow and the performance of a centrifugal compressor, CFD simulations and one-dimensional analyses have been carried out and several conclusions have been obtained as follows ;

(1) Secondary flow and loss factor defined with entropy generation have shown the characteristics of through-flow and loss mechanism of the tip leakage flow. The tip leakage vortex developed in the leading edge of the main blade passes over the next blade once more and makes up the high loss region at the impeller exit.

(2) The performance drop ($\Delta\pi/\pi^*$) and the efficiency drop ($\Delta\eta/\eta^*$) from the zero tip clearance have been decomposed into two components of the inviscid loss and the viscous loss. Two components have shown equal contribution to the performance loss, while the efficiency drop has been affected by the viscous loss alone. The performance drop and the efficiency drop have been proportional to the ratio of the tip clearance to the blade exit height (t/b_2): $\Delta\pi/\pi^* \approx 0.88t/b_2$, $\Delta\eta/\eta^* \approx 0.35t/b_2$.

(3) The tip leakage flow causes the flow blockage near the shroud and the slip velocity at the impeller exit. At small tip clearance, the flow blockage is more important than the slip velocity for the specific work.

(4) The additional entropy generation ($\Delta s - \Delta s^*$) due to the tip leakage flow agrees well with the kinetic energy of the tip leakage flow. This means that using Eqs. (10) and (12) makes the efficiency drop predictable without any correlation at the design stage.

Acknowledgment

The research was supported in part by grants from Seoul National University Mechanics Division of Brain Korea 21 and Dual Use Technology Program for the Civilian and Military Sector.

References

Choi, C. H., 1999, "Analysis of Steady and Unsteady Compressible Flows Using a Low Reynolds Number $k-w$ Turbulence Model," *Ph. D. Dissertation. Seoul National University, Korea.*

Cumpsty, N. A., 1989, *Compressor Aerodynamics*, Longman Scientific & Technical.

Denton, J. D., 1993, "Loss Mechanisms in Turbomachines," *Journal of Turbomachinery*, Vol. 115, pp. 621~656.

Farge, T. Z., Johnson, M. W. and Maksoud, T. M. A., 1989, "Tip Leakage in a Centrifugal Impeller," *Journal of Turbomachinery*, Vol. 111, pp. 224~249.

Hah, C. A., 1986, "A Numerical Modeling of Endwall and Tip-Clearance Flow of an Isolated Compressor Rotor," *Journal of Engineering for Gas Turbines and Power*, Vol. 108, pp. 15~21.

Ishida, M., Ueki, H. and Senoo, Y., 1990, "Effect of Blade Tip Configuration on Tip Clearance Loss of a Centrifugal Impeller," *Journal of Turbomachinery*, Vol. 112, pp. 14~18.

Japikse, D. and Baines, N. C., 1994, *Introduction to Turbomachinery*, Concepts ETI, Inc. and

Oxford University Press.

Koch, C. C. and Smith Jr., L. H., 1976, "Loss Sources and Magnitudes in Axial-Flow Compressors," *Journal of Engineering for Power*, July, pp. 411~424.

Lakshminarayana, B., 1970, "Methods of Predicting the Tip Clearance Effects in Axial Flow Turbomachines," *Journal of Basic Engineering*, Vol. 92, pp. 467~482.

Lakshminarayana, B., 1996, *Fluid Dynamics and Heat Transfer of Turbomachinery*, John Wiley & Sons, Inc.

Larosiliere, L. M., Skoch, G. J. and Prahst, P. S., 1999, "Tip Leakage in a Centrifugal Impeller Using Computational Fluid Dynamics and Measurements," *Journal of Propulsion and Power*, Vol. 15, No. 5, pp. 623~632.

Moore, J., Moore, J. G. and Timmis, P. H., 1984, "Performance Evaluation of Centrifugal Compressor Impellers Using Three-Dimensional Viscous Flow Calculations," *Journal of Engineering for Gas Turbines and Power*, Vol. 106, pp. 475~481.

Myong, H. K. and Yang, S. Y., 2003, "Numerical Study on Flow Characteristics at Blade Passage and Tip Clearance in a Linear Cascade of High Performance Turbine Blade," *KSME International Journal*, Vol. 17, No. 4, pp. 606~616.

Pampreen, R. C., 1973, "Small Turbomachinery Compressor and Fan Aerodynamics," *Journal of Engineering for Power*, July, pp. 251~256.

Rains, D. A., 1954, "Tip Clearance Flows in Axial Flow Compressors and Pumps," California Institute of Technology, Hydrodynamics and Mechanical Engineering Lab., Report No. 5.

Senoo, Y. and Ishida, M., 1986, "Pressure Loss Due to the Tip Clearance of Impeller Blades in Centrifugal and Axial Blowers," *Journal of Engineering for Gas Turbines and Power*, Vol. 108, pp. 32~37.

Senoo, Y. and Ishida, M., 1987, "Deterioration of Centrifugal Performance Due to Tip Clearance of Centrifugal Impellers," *Journal of Turbomachinery*, Vol. 109, pp. 55~61.

Shum, Y. K. P., Tan, C. S. and Cumpsty, N. A., 2000, "Impeller-Diffuser Interaction in Centrifugal Compressor," *Journal of Turbomachinery*, Vol. 122, pp. 777~786.

Storer, J. A. and Cumpsty, N. A., 1991, "Tip Leakage Flow Axial Compressor," *Journal of Turbomachinery*, Vol. 113, pp. 252~259.

Whitfield, A. and Baines, N. C., 1990, *Design of Radial Turbomachines*, Longman Scientific & Technical.